Patient-Specific 3D Scanned and 3D Printed Antimicrobial Polycaprolactone Wound Dressings

Zaid Muwaffak Hassan [a], Alvaro Goyanes [b], Vivienne Clark [a], Abdul W. Basit [a, b] Stephen T. Hilton [a], Simon Gaisford [a, b]

[a] UCL School of Pharmacy, University College London, 29-39 Brunswick Square, London, WC1N 1AX, UK

[b] FabRx Ltd., 3 Romney Road, Ashford, Kent TN24 0RW, UK

Corresponding authors:

Stephen Hilton

Simon Gaisford

s.hilton@ucl.ac.uk

s.gaisford@ucl.ac.uk

Abstract

The increasing prevalence of wound infections caused by antibiotic resistant bacteria is an urgent challenge facing modern medicine. To address this issue the expedient use of antimicrobial metals such as zinc, copper and silver were incorporated into an FDA-approved polymer (polycaprolactone - PCL) to produce filaments for 3D printing. These metals have broad-spectrum antimicrobial properties, and moreover, copper and zinc can enhance the wound healing process. 3D scanning was used to construct 3D models of a nose and ear to provide the opportunity to customize shape and size of a wound dressing to an individual patient. Hot melt extrusion was used to extrude pellets obtained by vacuum-drying of solutions of PCL and the different metals in order to manufacture metal-homogeneously-loaded filaments. Wound dressings with different shapes were produced with the filaments containing different concentrations of metals. Release of the metals from the dressings was determined by inductively coupled plasma atomic emission spectroscopy. All the different metal dressings show fast release (up to 24 h) followed by slow release (up to 72 h). The antibacterial efficacy of the wound dressings was tested using a thermal activity monitor system, revealing that silver and copper wound dressings had the most potent bactericidal properties. This study shows that 3D scanning and 3D printing, which are becoming simpler and more affordable, have the potential to offer solutions to produce personalised wound dressings.

Keywords:

3D printing

3D scanning

Wound dressings

Polycaprolactone

Additive manufacturing

Personalised medicine

1 Introduction

The skin is the largest organ in the body, functioning as a sensory system, regulating both temperature and moisture transmission and acts as a physical barrier against the external environment. When a wound occurs, due to trauma or disease, the barrier becomes compromised. This can increase the susceptibility of the wound site to microbial infections originating from endogenous sources, such as surrounding skin and mucous membranes, or from exogenous sources, such as those introduced by injury or from the local environment (Landis, 2008). The introduced microorganism may overcome the host's defences and invade into deeper tissues, progressing to a more severe infection, thus causing further damage and delaying healing of the wound (Siddiqui and Bernstein, 2010).

A wound may require the application of an external dressing to temporarily compensate for the damaged barrier and to allow healing to initiate and progress. A wound dressing isolates the injury site from the external environment, and provides an optimal environment for the wound to heal by promoting haemostasis and limiting tissue oedema through external compression (Zahedi et al., 2010). Wound dressings, traditionally used to protect the wound from contamination, can be used as platforms to deliver actives to wound sites. The use of solid wound dressings is preferred to the use of topical bioactive agents in the form of solutions, creams, and ointments in the case of exudative wounds for drug delivery to the wound as they provide better exudate management and prolonged residence at the wound site. These dressings are potentially useful in the treatment of local infections being beneficial to achieve increased local concentrations of antibiotics while avoiding systemic treatment, thus reducing patient exposure to an excess of drug beyond that required at the wound site (Boateng and Catanzano, 2015).

Due to the alarming increase of multi-drug resistance bacteria worldwide, caused by the over-use and miss-use of antibiotics, the application of broad-spectrum antimicrobial agents such as metal ions is an attractive target. Having been used historically for their antimicrobial properties(Lemire et al., 2013; Tenaud et al., 2009), the use of inorganic antimicrobial metals in the fight against infections is of high importance due to the fact that they act on multiple bacterial pathways, which makes it difficult for the bacteria to develop resistance against them (Huh and Kwon, 2011). Silver is probably the most commonly used metal, but zinc and copper, two of the essential trace elements in the human body, are also known to play an integral part in the wound healing process.

Silver ions have been shown to bind to various bacterial cell membrane proteins to cause cell lysis, and can be transported into bacterial cells, where silver ions disrupt the cell wall to interfere with energy production, enzyme function, cell replication and ultimately cell death (Chopra, 2007; Fong and Wood, 2006; Jain et al., 2009). There remains a concern in relation to the toxicity of silver to humans, however, most frequent side effects including local skin irritation, discolouration or staining which are harmless and usually reversible (Cutting et al., 2007). Copper ions function by altering proteins and inhibiting their biological activity, membrane lipid peroxidation, and plasma membrane permeabilization (Borkow and Gabbay, 2005; Gabbay et al., 2006). Copper can improve the healing process as it plays a key role in the enhancement of angiogenesis, via induction of vascular endothelial growth factor (VEGF), up-regulating the activity of copper-dependent enzymes, cell proliferation and re-epithelisation (Liu et al., 2009). It is suggested that the mode of action of ZnO is due to the disruption of bacterial cell membranes, and zinc is involved in several transcription factors and enzyme systems, stimulates the proliferation of epidermal cells, and increases collagen synthesis. Topical zinc can improve the healing of wounds especially in patients with zinc deficiency (Lemire et al., 2013), which can be a result of hereditary causes (Lansdown et al., 2007).

Wound dressings are usually prepared from absorbent, cross-linked polymer networks. One potential polymer is polycaprolactone (PCL), a semi-crystalline polyester that is biodegradable and biocompatible. These properties have led to the approval of several PCL drug-delivery devices and implants by the FDA (Salgado et al., 2012). It has a slow rate of degradation *in-vivo* compared with other biodegradable polyesters, a property that can be exploited in the manufacture of controlled release formulations (Li et al., 2014). PCL has been widely investigated in wound and burn dressings (Boateng et al., 2008; Ng et al., 2007), tissue engineering (Kweon et al., 2003), scaffold manufacturing (Kamath et al., 2014) and drug targeting (Freiberg and Zhu, 2004).

Three-dimensional printing (3DP) is a recently developed technology with numerous possibilities for the manufacture of medical devices. 3DP is an additive manufacturing process that allows the fabrication of three dimensional solid objects of virtually any shape. Of the several types of 3D printing, fused deposition modelling (FDM) has been most widely used for medical devices as it is simple, cost effective and extrudes polymer strands (Goyanes et al., 2016a; Yu et al., 2008). The printer feedstock is a thermoplastic filament that is heated to its softening point and then extruded through a print-head (driven by an X – Y orientation system) layer by layer over a build plate. The build plate is then lowered to a predetermined height and the process is repeated until the 3D object has been constructed. FDM 3DP has been used in various fields, such as tissue engineering, scaffold manufacturing (Fielding et al., 2012), and to produce oral drug delivery formulations (Goyanes et al., 2014; Goyanes et al., 2015a; Goyanes et al., 2016b; Goyanes et al., 2015b; Melocchi et al., 2015; Pietrzak et al., 2015). The 'instructions' for the 3D printer on how to build the object comes from the printer's software that slices the source digital file into layers that form the instructions for the 3D printer. This digital file can be created using computer-aided design software, to construct a new 3D object, or with the use of 3D scanning, to copy an existing object. 3D scanning is a non-contact, non-destructive technology that digitally captures the shape of physical objects with a 3D scanner using laser light that collects distance information from surfaces. This information is then used to create 'point clouds' of data from the surface of the object. Hence, 3D laser scanning is a way to capture a physical object's exact size and shape to construct a 3D model (Koch, 2012). The proof of concept of combining 3D printing and 3D scanning for the manufacture of antiacne masks/patches has been previously reported (Goyanes et al., 2016a), whereas the use of FDM printing showed high drug degradation due to the heating process while printing.

The combination of 3D printing and 3D scanning could possibly revolutionise patient care by allowing custom-manufacture of devices for individual patients and it is the exploration of this concept, applied specifically to wound dressings, that is the focus of this work. Hot melt extrusion was used to incorporate metal ions into a PCL filament and the 3D printer was used to fabricate dressings against scanned templates of a target wound. The antimicrobial efficacy of the dressings was also assessed using an *in-vitro* assay.

2 Materials and Methods

2.1 Materials

PCL pellets ($(C_6H_{10}O_2)n$, Mw $\sim$ 80,000) and silver nitrate ($AgNO_3$) were purchased from Sigma-Aldrich, UK. Copper sulphate (II) pentahydrate ($CuSO_4 \cdot 5H_2O$) was purchased from VWR chemicals, Belgium. Zinc oxide (ZnO) was purchased from Alfa Aesar, USA. The test organism *Staphylococcus aureus* (NCIMB 9518) was purchased from Fisher Scientific, UK. Nutrient broth (CM0001) was purchased from Thermo Scientific, UK.

2.2 Methods

2.2.1 Preparation of metal loaded filaments

- Silver-loaded filament (10% loading w/w):

$AgNO_3$ (3 g) was dissolved in 10 mL of deionized water using a magnetic stirrer. Tetrahydrofuran (THF, 200 mL) was added to the silver solution under stirring. Finally, 27g of PCL pellets was then added to the solution and the mixture was stirred at 40 °C until complete dissolution of PCL. The solvents were removed with a rotary evaporator under reduced pressure at 40 °C for 2 h followed by high-vacuum drying for 1h. The dried material ($AgNO_3$ homogeneously distributed in the PCL) was chopped into pellets and extruded with Filabot filament hot-melt extruder (Filabot Inc, USA) with a single screw and a 1.75 mm nozzle head. The extrusion temperature was 80 °C.

- Copper-loaded filament (10 and 25% loading w/w):

$CuSO_4 \cdot 5H_2O$ (3g or 7.5g for 10% or 25% loading respectively) was dissolved in 100mL methanol using a magnetic stirrer. PCL pellets (27 g or 22.5 g for 10% or 25% copper loading respectively) was then added to the copper solution, followed by 100mL dichloromethane (DCM) and the mixture was stirred at 40°C until complete dissolution of PCL. A rotary evaporator (under reduced pressure) was used to evaporate the solvents at 40 °C for 3 h followed by high-vacuum drying for 1 h. The dried material ($CuSO_4$ homogeneously distributed in the PCL) was chopped into pellets and extruded with Filabot filament hot-melt extruder (Filabot Inc, USA) with a single screw and a 1.75mm nozzle head. The extrusion temperature was 60°C.

- Zinc-loaded filament (10 and 25% loading w/w):

ZnO (3g or 7.5g for 10% or 25% zinc loading respectively) was dissolved in 100 mL ethanol using a magnetic stirrer. PCL pellets (27g or 22.5g for 10% or 25% copper loading respectively) was added followed by 100 mL DCM and the mixture was stirred at 40°C until complete dissolution of PCL. The solvents were removed using a rotary evaporator at 40 °C for 3 h followed by one hour high-vacuum drying. The dried material (ZnO homogeneously distributed in the PCL) was chopped into pellets and extruded with Filabot filament hot-melt extruder (Filabot Inc, USA) with a single screw and a 1.75mm nozzle head. The extrusion temperature was 75°C.

For all the filaments prepared the diameter of the filament was checked using a digital calliper throughout the extrusion process, since it is important to get a consistent filament diameter within an acceptable range for the 3D printer.

2.2.2 3D Scanning

3D scans were captured with a Sense 3D Scanner (3D Systems, USA). It functions by capture of the surface data of a physical object reflected light from a laser. In this work, scans were captured of a nose and ear, because 3D printed dressings of these body parts can dress anatomically complex areas compared to conventional flat dressing, what would provide more comfort to the patient. The settings used were high resolution, with object recognition enabled, colour scanning and landscape orientation. The person being scanned was in a setting position, while the person holding the 3D scanner was rotating 360°around the subject while maintaining about 40 cm distance to the subbject. These 3D scans were cut, optimized for 3D printing and templates were made using Autodesk Meshmixer 10.8.

2.2.3 3D Printing

A MakerBot Replicator 2X Desktop 3D printer (MakerBot Inc., USA) was used to print wound dressings shaped to match the nose and ear scans, in addition to square dressings (20 x 20 x 1 mm) for antimicrobial studies and circular dressings (10 mm diameter x 1 mm thickness) for dissolution testing. The templates for the square and circular dressings were created using Tinkercad (Autodesk) – a browser-based 3D design and modelling tool.

The nozzle head was cleaned (for 20 – 25 s) prior to printing the metal-loaded filaments, and between prints containing different metal ions or different concentrations, by extruding plain PCL filament. The settings of the printer, which will ultimately determine how the 3DP dressings will turn out, were selected based on preliminary results with the metal loaded filaments. All the dressings were printed at an extrusion temperature of 170 °C, high resolution (0.1 mm layer height), with two shells, 100% infill and speed while extruding and while travelling was set to 50 mm/s. A raft and support were used for the printing of the nose and ear dressings, while no support or raft was used for the printing of the flat dressings printed for analytical purposes.

2.2.4 Thermal characterisation of metal-loaded filaments and dressings

Differential scanning calorimetry (DSC): Measurements of the metal loaded filaments and the 3D printed dressings were performed using a TA Q2000 DSC (TA Instruments LLC, USA), calibrated with indium (T_m = 156.6 °C, ΔHf = 28.71 J/g). Nitrogen gas was used as a purge with a flow rate of 50 mL/min. Tzero hermetic pans with lids were used for all samples, with an average sample weight of 7-9 mg. Samples were cooled to -80 °C then heated to 200 °C at a heating rate of 10 °C/min.

Thermogravimetric analysis (TGA): TGA analysis was performed with TA Discovery TGA (TA Instruments LLC, USA) with nitrogen as purge (flow rate = 25 mL/min). Open aluminium pans were used, and samples were heated from room temperature (15 ± 0.5 °C) to 200 °C at 10 °C/min.

2.2.5 Scanning electron microscopy (SEM)

Surface and cross-section images of the filaments were taken using JSM-840A Scanning Microscope, JEOL GmbH, Germany. The voltage and working distance were set at 5 kV and 50 mm, respectively. Filament samples were placed on double-sided carbon tape, mounted on stubs and sputter coated using a Polaron E5000 machine with Au/Pd. Samples were coated for 1 minute prior to imaging.

2.2.6 Fourier transform infrared (FTIR) spectroscopy

FTIR spectra of Ag, Cu and Zn powder, filaments and dressings were acquired using Bruker ALPHA Platinum FT-IR spectrometer (USA) to determine if Ag, Cu or Zn form any bonding with the polycaprolactone matrix. Spectra were acquired at 4000 cm^{-1} to 400 cm^{-1} and a resolution of 2 cm^{-1}.

2.2.7 Dissolution testing of wound dressings

For each assay the dressing was placed into a sterile 10 mL vial with agitation in the dissolution medium (10 mL of 0.1 M phosphate buffer – pH 7.4). The vials were capped and incubated in a thermostated bath at 37 °C for three days. At regular intervals (0, 6, 12, 18, 24, 36, 48, 60 and 72 h), 1 mL aliquots were sampled from each vial and replaced with an equal amount of phosphate buffer. The samples were then diluted to 5 mL with 96% (w/w) nitric acid (to digest any dissolved polymer matrix), stirred at room temperature for 1 h, then 1 mL was taken from that solution and diluted further to 20 mL with phosphate buffer.

Analysis of the samples was performed with Inductively Coupled Plasma Atomic Emission Spectroscopy (ICP-AES) using an Axial Varian 720-ES, with argon as a purge gas. Ag was analysed at wavelength 328.068 nm, Cu at 327.395 nm and Zn at 213.857 nm. A second wavelength (338.289 nm for Ag, 324.754 nm for Cu and 202.548 nm for Zn) was used to confirm the reproducibility of the results. Each dressing was tested in triplicate and the mean value determined.

2.2.8 Antibacterial efficacy of wound dressings

Antibacterial efficacy of wound dressings was tested against *S. aureus* which is a common bacterium to causes skin infections. *S. aureus*, stored in 1 mL aliquots at -80 °C in 15% w/v glycerol, was defrosted at 37 °C and used to inoculate nutrient broth, which was incubated overnight aerobically at 37 °C. Bacteria were harvested from the broth by centrifugation at 3000 g for 10 min and washed in phosphate buffered saline (PBS) (Fisher Scientific, UK) three times. The resulting bacterial suspension was adjusted to a 0.5 McFarland standard using PBS to standardize the cell numbers to approximately 1 x 10^8 cfu/mL. This was verified with serial dilution and spread plating.

Dressing samples (plain PCL, Ag-PCL, Cu-PCL, and Zn-PCL) printed with identical settings (see 3D printing above) were cut to the required weights (10, 20, 25, 30, 40, 50, 75 and 100 mg) immediately prior to use and inserted into a sterile 3 ml calorimetric ampoule (Hichrom, UK). Nutrient broth (2.97 mL) was added to the ampoule, followed by inoculation with the bacterial suspension (30 µL). The ampoule was then sealed with a crimp cap. A control ampoule was prepared for each experiment containing only nutrient broth and the same inoculum of bacteria. The ampoule was vortexed briefly before being transferred to a 2277 Thermal Activity Monitor (TAM, TA Instruments Ltd, UK).

The ampoules were allowed to equilibrate for up to 30 min before being lowered into the measuring position of the TAM (set at 37 °C with an amplifier setting of 1000 µW). Digitam 4.1 software collected heat output data every 10 s for 48 h.

After calorimetric analysis, ampoules were removed from the TAM and inspected for turbidity. Non-turbid ampoules were vortexed for 10 s then opened and 1 mL of nutrient broth removed to enumerate the bacteria. The sample was centrifuged at 3000 g for 10 min and resuspended in PBS three times in an attempt to remove any metal ions that could affect the growth of the bacteria on agar. The resulting bacterial suspension underwent serial dilution and spread plating on ISA, followed by incubation overnight at 37 °C. Colonies were counted, and the number of viable bacteria in the ampoule calculated.

3 Results and Discussion

The manufacture of metal-loaded filaments for 3D printing was achieved with PCL. Five metal loaded PCL filaments were produced with different concentrations: Ag (10% w/w)-PCL, Zn (10% w/w)-PCL, Zn (25% w/w)-PCL, Cu (10% w/w)-PCL and Cu (25% w/w)-PCL (Figure 1). The average filament diameter was 1.77 ± 0.3mm. The metal compounds and the PCL were dissolved in an appropriate solvent mixture and the solution vacuum-dried to obtain pellets with a homogeneously distribution of the metal compound into the PCL.

One of the most challenging parts of the process was the determination of a common solvent to dissolve both the metal and polymer. For instance, $CuSO_4 \cdot 5H_2O$ and $AgNO_3$ were soluble in water while ZnO and PCL were insoluble in water. It was established that a single solvent was not adequate to dissolve both the polymer and any of the metals so ultimately a combination of solvents was used to dissolve PCL and the metals (see Methods for the exact combination for each preparation). This method is cheap, versatile and only requires the selection of suitable solvents, moreover the direct extrusion of the metal compounds and PCL is not recommended since that lead to filaments with a very poor distribution of the metal compounds in the PCL.

Two factors were critical in ensuring extrusion produced a filament of consistent diameter. Firstly, the extrusion temperature varied depending on the mixture content and how dry the mixture was. Copper-containing mixtures required a lower extrusion temperature (60 °C) compared with the non-copper-containing mixtures (which were extruded at 75 – 80 °C). This could be due to the lower melting temperature of $CuSO_4 \cdot 5H_2O$ (110 °C) compared with $AgNO_3$ (212 °C) and ZnO (1975 °C). When the extrusion temperature was lower than required, it led to a thicker filament and/or clogging of the extruder. Higher extrusion temperatures led to the extrusion of filaments that were thin and inconsistent (about 1.35 ± 0.05 mm). Secondly, a regular feeding rate was required to produce a uniform filament diameter.

SEM micrographs of the filaments revealed that all the filaments had homogenous and uniform surface and cross section, indicating uniform metal distribution inside the filaments (Figure 2).

3D templates for wound dressings were successfully obtained from 3D scanning. The resolution of the 3D scanner was one of the main factors determining the quality of the 3D scans, however, lighting conditions (e.g. direct sunlight) and room temperature did affect the depth of acquisition of the scanner.

Ag, Cu and Zn loaded PCL dressings were printed. Figure 3 shows an example of a Cu-PCL printed nose dressing (see Appendix 1 for more examples). All the dressings were flexible, most likely due to the elastomeric properties of PCL. These 3D printed dressings have an advantage over conventional flat dressing in that they can dress anatomically complex areas. This would provide more comfort to the patient and improve adherence. The cytocompatibility of PCL in addition to the possibility of incorporating bioactive or antimicrobial agents means that PCL has the potential to be tailored into an effective wound dressing with appropriate bio-physical properties (e.g. vapour permeability and flexibility) and personalised shape and size. The use of metal ions improves the printing performance of the PCL filaments. In a previous study using PCL filaments loaded with salicylic acid for the treatment of acne, the 3D printer was able to manufacture flat disc/patches but not complex shapes as personal shape devices (Goyanes et al., 2016a).

FTIR spectra of plain PCL pellets (before 3D printing) exhibited both absorption bands of the –C–H and C=O functional groups at 2942 cm^{-1} and 1722 cm^{-1} respectively (Figure 4). FTIR analysis of the printed plain PCL, Ag(10%)-PCL, Cu(10%)-PCL, Cu(25%)-PCL, Zn(10%)-PCL and Zn (10%)-PCL showed all absorption bands of the functional groups (–C–H and C=O). In addition, there was no shift in peak positions of the metal-loaded 3D printed samples compared to plain PCL pellets or 3D printed PCL, indicating that there was no chemical bonding between PCL, Ag, Cu or Zn had occurred during extrusion and printing of the dressings.

The main limiting factor in printing good dressings was a consistent filament diameter within an acceptable range for the 3D printer. A filament thin in sections resulted in areas of the dressings containing less material than other areas, and thicker filament sections were too difficult for the

extruder head to grip. Thus, after various experimentations with slight variations in filament diameters, it was determined that the consistency of the filament diameter (1.69 – 1.77 mm) was more important than the size of the diameter (given that it is within acceptable range of the 3D printer; 1.60 – 1.79 mm).

3D printing of wound dressings of good quality requires an understanding of the settings that will ultimately dictate how they would turn out. For dressings printed in this work, these settings were the layer height, number of outer shells and both speed while extruding and travelling. These settings, individually or combined, did directly control the surface finish, density and quality of the final print.

Increasing the number of shells (the outer most layers of the print) provided stronger dressings; however, they increased printing time and reduced quality (e.g. 4 shells resulted in substantial reduction of details and inconsistent surface of printed dressings compared to 2 shells). Having too few shells resulted in a weak and fragile print. There needs to be a balance between not having enough or too many shells, and in this case, the default of two outer shells was a good compromise.

The resolution of the 3D printed dressing is determined by the layer height. Using a smaller layer height provided a considerable increase in detail and increased printing time. The MakerBot Replicator 2X can print in layer heights between 0.1 mm and 0.3 mm, however it was only possible to obtain good quality prints with 0.1 mm layer heights. One reason for this is because 3D prints made with FDM printers typically have visible ridges between different layers, and a smaller layer height helps to reduce (but not eliminate) them.

The printing temperature in addition to both printing and movement speed determine if it is possible to print at all. The extrusion temperature depends on the filament material being used, for instance, plain PCL dressings could be printed with as low as 140 °C. However, when PCL is loaded with metals, it was not possible to print until this temperature was increased to 170 °C. High movement speed while printing or travelling reduced the printing time by making the print-head move faster, but resulted in poorer print quality. On the other hand, slower speed meant that the hot print-head would stay longer above the extruded layers resulting in burnt layers, especially the last layers. The optimal settings found in this case was 50 mm/s for both printing and travelling speeds.

The DSC thermogram (Figure 5) shows that plain PCL dressing has a melting temperature (T_m) of 60.9°C and a glass transition temperature (T_g) of -63.4 °C which agrees with the literature values of PCL pellets (60.0 °C and -60.0 °C respectively) (Hutmacher et al., 2001). All the metal loaded dressings show similar thermal profiles compared with the plain PCL dressing without any degradation at temperatures up to 200 °C. Ag-PCL had the lowest T_m (59.4 °C) while Zn-PCL had the highest (61.8 °C). Ag-PCL dressing decreased the T_m while both Zn-PCL and Cu-PCL dressings increased it slightly, these changes did not have effect on the printability of the filaments.

TGA showed no significant mass loss (0.44% to 1.89%), most likely due to loss of residual solvents. Copper-containing dressings (10 and 25% w/w) showed the highest amount of weight loss (1.63% and 1.89% respectively) compared with the other dressings. This could be due to the hygroscopicity of copper sulphate. This might become an issue in the future during storage and transport of the dressings. However, with proper storage conditions and packing this concern can be overcome.

Thus it can be concluded that the thermal analysis results confirm that the printed dressings were stable and that the printing and extrusion processes did not affect the properties of PCL. It is

important to note that even though the residence time of the formulation in the print head is short (a few seconds), thermally labile formulations may experience some degree of degradation during the printing process (Goyanes et al., 2016a). Hence, DSC analysis may be used to assess the suitability of the formulation for FDM 3D printing (Goyanes et al., 2015a).

One of the challenges in antimicrobial research for wound dressings is achieving sustained release of the antimicrobial agent for extended prevention of bacterial infection. The release of Ag, Cu and Zn from PCL dressings to the surrounding environment is shown in Figure 6. During the first 24 h of the experiment, Ag was released very quickly (40.69 μg/mL), but the release rate decreased rapidly in the following 24 h reaching a concentration of 44.53 μg/mL at 48h. From 48 to 72 h the concentration of Ag remained almost constant at 45.85 ± 1.10 μg/mL. The fast release observed in the first 24 h is most likely the release of Ag from the surface of the PCL matrix, and the slower release afterwards is due to the slow diffusion of Ag from the interior of the polymer matrix to the surface before release. The final concentration (44.53 μg/mL) is two folds higher than the minimum inhibitory concentration and minimum bactericidal concentration previously reported for silver against *S. aureus* (22.083 μg/mL) (Said et al. 2014).

Over the same time period (0 – 72 h) the concentration of Cu and Zn had the same trend but was always much lower compared to Ag. The release rate was highest for 10% Ag-PCL (45.85 μg/mL) and lowest for 10% Zn-PCL (15.87 μg/mL). Both 25% Cu-PCL and 25% Zn-PCL had higher release rate compared to their corresponding 10% dressings. This is due to the fact that the metal content in the 25% dressing is higher than the 10% leading to more metal being released. 25% Cu-PCL had higher release rate than 25% Zn-PCL (same applies for the 10% dressings of both metals). Minimum inhibitory concentration for copper against *S. aureus* was reported to be between -3 – 40 μg/ml, being the minimum bactericidal concentration between 7 and 60 μg/ml (Argueta-Figueroa et al. 2014). The amount of copper released from the dressings was 17.756 μg/ml (for 10%) and 26.634 (for 25%), values which fall in the middle of the reported values. However, the antibacterial efficacy of Zn and Cu is dependent on the concentration of the metal, the initial bacterial concentration, and the strains of bacteria employed in the study.
The minimum inhibitory concentrations found in the literature for Zn against *S. aureus* are very variable and not comparable to the test performed in this study. Zn nanoparticles vs *S. aureus* showed a minimum inhibitory concentration determined by agar dilution method of 625 μg/ml (Aleaghil et al. 2016). The highest concentrations obtained were 15.87 μg/ml for 10% and 20.63 μg/ml for 25% Zn wound dressings, which are significantly lower than the concentration reported.

The controlled release of Ag, Cu and Zn from PCL dressings is attributed to the entrapment of the metals into PCL, which acts as a barrier for the release of these metals from the dressing due to the slow water penetration into the PCL matrix. These results confirm that entrapment of metal ions into PCL dressings delays the release of the metals. This is desirable to maintain sufficient release of antimicrobial agent to remain active for the duration of treatment, while preventing high concentrations to be released upon initial application which would prevent adverse events (such as irritation) from high doses. Another advantage of a slower and prolonged release rate of Ag, Zn and Cu in clinical practice is that it would reduce the number of dressing changes, which can be very painful (Meaume et al., 2004).

These results are in agreement with the solubility of the metals in water (majority constituent of the phosphate buffer testing medium) where Ag has superior solubility properties, followed by Cu then Zn. Ideally, the dissolution testing could have been performed in the same medium used in the

antibacterial testing. This could give a better correlation between release profiles of the metals from dressings and antibacterial activity. However, that was not possible as the nutrient broth used for antibacterial testing contains NaCl which led to the precipitation of solid AgCl when Ag-PCL dressing was dissolved in the medium during the initial experiments. Moreover, pH 7.4 of the phosphate buffer resembles the pH at surface of the skin providing closer correlation to the *in-vivo* environment.

Isothermal micro-calorimetry (IMC) was used to quantitatively monitor the efficacy of silver, zinc and copper in wound dressings. IMC monitors the rate of heat production (power) in a sample, where the power signal is proportional to the number of viable cells in the sample. This allows for real-time measurement of the growth (or inhibition) of *S. aureus*, without being affected by non-viable cells. This method is not dependent on optical clarity (which can be effected by the presence of the metal ions in the sample), and does not require the organism to be removed from its environment to be sampled (Gaisford et al., 2009; O'Neill et al., 2003). The drawback of IMC is that because heat is absorbed or produced by different events occurring in the sample, could mean that the power signal measured is potentially a combination of several processes. However, a careful experimental design can improve these issues as discussed by S. Gaisford et al. (Gaisford, 2005).

The control experiments of *S. aureus* (without any dressing or metals) shows a characteristically complex pattern, exhibiting an exponential growth phase in the first few hours with two distinctive biphasic peaks, during which heat is generated and an increase in power is recorded (Figure 7A). The area under the curve (AUC – total heat output) of the controls is reproducible (n = 3) to 3.5%. As discussed by Zaharia et al. (2013), the first exponential phase (0 – 3 h) represents aerobic metabolism where the available oxygen (blue arrow in Figure 7A), dissolved in the medium is utilised (the ampoules are sealed but not completely filled to the top). This is then followed by a change in aerobic metabolism (3 – 10 h) using diffused oxygen from the head space of the ampoule (red arrow in Figure 7A). The last peak of the thermogram represents anaerobic metabolism of the organism using any remaining carbon sources that the organism is able to metabolise (green arrow in Figure 7A) (Zaharia et al., 2013). The exhaustion of nutrients, pH drift and the appearance of toxic metabolites consequently stopping the organism from growing anymore. This resulted in the power signal to return to baseline (zero) and hence decided the 48 hour duration of the experiment.

In the presence of plain 3D PCL dressings (i.e. the dressings with no antimicrobial metal agent), PCL showed no effect on the initial aerobic phase and the overall growth is very similar to that of the control (Figure 7B). There was very slight variation in the second growth phase which was attributed to microorganism cells becoming entrapped within the PCL dressing. Therefore, diffusion of medium to those trapped cells and metabolites from those microorganisms to the medium will be different compared to those present in the surrounding medium only. Thus, it can be concluded that PCL does not have any intrinsic antimicrobial properties, and increasing amounts of PCL does not affect the growth of *S. aureus*.

The shape of the growth curve is significantly different in the presence of 10% (w/w) Ag-PCL dressing (Figure 7C). Use of 10 mg of Ag-PCL dressing delayed the growth by *ca.* 16 h, and inhibition of growth was observed when larger masses (20, 30 and 40 mg) were used when compared to the control. Viable counts at the end of each experiment (Table 1) confirmed a bactericidal effect on the bacteria, with a three log reduction in bacteria compared to the inoculum. These results indicate that silver dressing is effective at inhibiting the growth of *S. aureus* via a bactericidal mechanism, and that increasing amount of silver causes a more potent inhibition.

Table 1. Viable cell counts after the IMC study

Formulation			10% Ag - PCL		
Mass of the dressing	Control (0g)	10 mg	20 mg	30 mg	40 mg
Viable cells	140,333	105	20	0	0
Formulation			10% Cu - PCL		
Mass of the dressing	Control (0g)	25 mg	50 mg	75 mg	100 mg
Viable cells	121,667	120,311	95,038	56,664	51,682
Formulation			25% Cu - PCL		
Mass of the dressing	Control (0g)	25 mg	50 mg	75 mg	100 mg
Viable cells	120,660	14,738	1,202	220	48
Formulation			10% Zn - PCL		
Mass of the dressing	Control (0g)	25 mg	50 mg	75 mg	100 mg
Viable cells	119,333	117,855	117,439	111,538	89,795
Formulation			25% Zn - PCL		
Mass of the dressing	Control (0g)	10 mg	20 mg	30 mg	40 mg
Viable cells	119,916	84,764	81,297	71,859	68,315

Figure 7D shows the corresponding growth curves for *S. aureus* in the presence of increasing masses of 10% (w/w) Cu-PCL. All the samples (10 – 40 mg) showed no inhibition of the microorganism. This indicates that at this concentration Cu is ineffective at inhibiting the growth of S. aureus after 48 h, due to a slow release rate or the concentration of Cu is not sufficient. Hence, 25% (w/w) Cu-PCL was tested to determine if there is any improvement with higher concentrations of Cu (Figure 7E). Several differences from the control are apparent, but the interpretation of these data is difficult. There is an absence of any of the characteristic growth peaks of *S. aureus*, with high-power peaks at the beginning with an immediate sharp decline in power instead. There was no growth in any of the samples, which was confirmed by the non-turbidity of all the samples after the TAM experiments. In addition, viable counts revealed that a 25 mg dressing showed a two log reduction in viable bacteria (while higher masses of the dressing had stronger inhibition) at the end of the TAM experiment compared to the initial inoculum (Table 1). This suggests that Cu is effective at inhibiting the growth of *S. aureus*, although higher concentrations are required compared to silver. In efforts to explain

the unusually high peaks at the start of the growth curves are due to Cu, the bacteria or an interaction between any of dressings' content's and that of the medium, copper sulphate powder only (without any bacteria or PCL) was tested exactly as the Cu-PCL dressing in water and broth. As can be seen in Figure 7F, both curves show a similar pattern to that of the 25% (w/w) Cu-PCL. This confirms that these peaks are due to copper sulphate powder and are not due to any interaction between the dressing content, bacteria or the medium.

Both 25 and 50 mg of 10% (w/w) Zn-PCL dressing showed no effect on the growth of *S. aureus* after 72 h (Figure 7G). While 75 mg and 100 mg of the dressing showed a small reduction in the intensity of the growth peaks, and a minor delay of the growth. These results suggest that at these concentrations Zn is ineffective at inhibiting the growth of *S. aureus*, as confirmed by cell counting (Table 1).

The results with 25% (w/w) Zn-PCL show stronger inhibition compared to the 10% (w/w) Zn-PCL dressing (Figure 7H). Both 10 and 20 mg of 25% Zn-PCL showed similar inhibition, which was weaker compared to 30 and 40 mg of the dressing. In addition, there was a time delay of the growth (34 – 82 min). These results suggest that increasing the concentration of Zn to 25% (w/w) increases the inhibition, however, it is not as effective as Ag or Cu. This is most likely due to a weaker bactericidal efficacy and lower release rate of Zn compared to Ag and Cu. Consequently, higher amounts of Zn may be required to be incorporated into the dressing to compensate for the low release rate and efficacy to achieve similar inhibition of Cu or Ag. This may present certain difficulties during formulation and an increase in cost. However, this may not be required as Zn can be incorporated into the dressing to benefit from its healing properties (especially in patients with zinc deficiency), in addition to the weaker antimicrobial efficacy.

It is important to make some clarifications regarding the nature of the assay method (IMC) used in this work. Any *in vitro* method will differ from the *in vivo* event, and the relevancy of these differences will depend on how the data is used. In this case, the *in vivo* environment is extremely difficult to reproduce. In a wound environment, bacteria can grow as biofilms or micro-colonies rather than planktonic cultures which can influence the susceptibility of the microorganism to an antibacterial agent (James et al., 2008). For instance, it has been suggested that the bactericidal concentration of silver required to eradicate biofilms of *Pseudomonas aeruginosa* is 10 to 100 fold higher than what is required to eradicate planktonic bacteria (Bjarnsholt et al., 2007). This would suggest that the concentrations used in this work might need to be increased to eradicate biofilms, since in the experiments reported here, the organism is growing in planktonic culture. In addition, the antimicrobial effect of metal ions is known to be strain dependent (Ruparelia et al., 2008). It is important to note that the metal release would be lower in skin versus suspending solution, although the release could be promoted increasing the metal loading in the filaments, so in the 3D printed wound dressings as shown in the ICP data. It is already reported that increasing the drug loading in 3D printed formulations increased drug release since there is less matrix compound (in this case PCL) avoiding the release of the active compounds (Goyanes et al., 2016b). The main aim of the microbiology experiments was to evaluate the efficacy of the metal loaded PCL wound dressings against a known skin pathogen (*S. aureus*), and to gain insights on how 3D printing might influence the outcome.

Since optimal moisture content maintains the vitality of tissue and promotes wound healing, theoretically, it would be possible to modify the thickness of the wounds dressings or to create regions with small gaps between the layers to modify the vapour permeability.

4 Conclusion

529 The results clearly demonstrate the utility of hot melt extrusion as a novel method to incorporate
530 antimicrobial Ag, Cu and Zn into polycaprolactone filaments that allow the 3D printing of
531 personalised wound dressings. 3D printed dressings demonstrated a clear advantage over
532 conventional flat dressings as they are anatomically adaptable. This method takes advantage of 3D
533 scanning to create 3D models of body parts which are then 3D printed in a personalised therapy. Ag-
534 PCL and Cu-PCL dressings showed the most bactericidal properties against *S. aureus* which is a
535 common bacterium to causes skin infections. This study therefore demonstrates a simple method to
536 produce customizable wound dressings that can be tailored to individual patients in regards to
537 shape, size and antimicrobial agents.

538

539 **5 Acknowledgment**

540 The authors wish to thank Professor John McArthur (Earth Sciences, UCL) for his advice and
541 assistance with the ICP-AES machine.

542

6 References

Bjarnsholt, T., Kirketerp-Møller, K., Kristiansen, S., Phipps, R., Nielsen, A.K., Jensen, P.Ø., Høiby, N., Givskov, M., 2007. Silver against Pseudomonas aeruginosa biofilms. Apmis 115, 921-928.

Boateng, J., Catanzano, O., 2015. Advanced Therapeutic Dressings for Effective Wound Healing--A Review. J. Pharm. Sci. 104, 3653-3680.

Boateng, J.S., Matthews, K.H., Stevens, H.N., Eccleston, G.M., 2008. Wound healing dressings and drug delivery systems: a review. J. Pharm. Sci. 97, 2892-2923.

Borkow, G., Gabbay, J., 2005. Copper as a biocidal tool. Curr. Med. Chem. 12, 2163-2175.

Chopra, I., 2007. The increasing use of silver-based products as antimicrobial agents: a useful development or a cause for concern? J. Antimicrob. Chemother. 59, 587-590.

Fielding, G.A., Bandyopadhyay, A., Bose, S., 2012. Effects of silica and zinc oxide doping on mechanical and biological properties of 3D printed tricalcium phosphate tissue engineering scaffolds. Dent. Mater. 28, 113-122.

Fong, J., Wood, F., 2006. Nanocrystalline silver dressings in wound management: a review. Int. J. Nanomedicine 1, 441.

Freiberg, S., Zhu, X., 2004. Polymer microspheres for controlled drug release. Int. J. Pharm. 282, 1-18.

Gabbay, J., Borkow, G., Mishal, J., Magen, E., Zatcoff, R., Shemer-Avni, Y., 2006. Copper oxide impregnated textiles with potent biocidal activities. J. Ind. Text 35, 323-335.

Gaisford, S., 2005. Stability assessment of pharmaceuticals and biopharmaceuticals by isothermal calorimetry. Curr. Pharm. Biotechnol 6, 181-191.

Gaisford, S., Beezer, A.E., Bishop, A.H., Walker, M., Parsons, D., 2009. An in vitro method for the quantitative determination of the antimicrobial efficacy of silver-containing wound dressings. Int. J. Pharm. 366, 111-116.

Goyanes, A., Buanz, A.B., Basit, A.W., Gaisford, S., 2014. Fused-filament 3D printing (3DP) for fabrication of tablets. Int. J. Pharm. 476, 88-92.

Goyanes, A., Buanz, A.B., Hatton, G.B., Gaisford, S., Basit, A.W., 2015a. 3D printing of modified-release aminosalicylate (4-ASA and 5-ASA) tablets. Eur. J. Pharm. Biopharm. 89, 157-162.

Goyanes, A., Det-Amornrat, U., Wang, J., Basit, A.W., Gaisford, S., 2016a. 3D scanning and 3D printing as innovative technologies for fabricating personalized topical drug delivery systems. J. Control. Release. 234, 41-48.

Goyanes, A., Kobayashi, M., Martinez-Pacheco, R., Gaisford, S., Basit, A.W., 2016b. Fused-filament 3D printing of drug products: Microstructure analysis and drug release characteristics of PVA-based caplets. Int. J. Pharm. 514, 290-295.

578 Goyanes, A., Wang, J., Buanz, A., Martinez-Pacheco, R., Telford, R., Gaisford, S., Basit, A.W., 2015b.
579 3D Printing of Medicines: Engineering Novel Oral Devices with Unique Design and Drug Release
580 Characteristics. Mol. Pharm. 12, 4077-4084.

581 Huh, A.J., Kwon, Y.J., 2011. "Nanoantibiotics": A new paradigm for treating infectious diseases using
582 nanomaterials in the antibiotics resistant era. J. Control. Release. 156, 128-145.

583 Hutmacher, D.W., Schantz, T., Zein, I., Ng, K.W., Teoh, S.H., Tan, K.C., 2001. Mechanical properties
584 and cell cultural response of polycaprolactone scaffolds designed and fabricated via fused deposition
585 modeling. J. Biomed. Mater. Res. 55, 203-216.

586 Jain, J., Arora, S., Rajwade, J.M., Omray, P., Khandelwal, S., Paknikar, K.M., 2009. Silver nanoparticles
587 in therapeutics: development of an antimicrobial gel formulation for topical use. Mol. Pharm. 6,
588 1388-1401.

589 James, G.A., Swogger, E., Wolcott, R., Secor, P., Sestrich, J., Costerton, J.W., Stewart, P.S., 2008.
590 Biofilms in chronic wounds. Wound Repair Regen. 16, 37-44.

591 Kamath, M.S., Ahmed, S.S., Dhanasekaran, M., Santosh, S.W., 2014. Polycaprolactone scaffold
592 engineered for sustained release of resveratrol: therapeutic enhancement in bone tissue
593 engineering. Int. J. Nanomedicine 9, 183-195.

594 Koch, M., 2012. 3D scanner - Unabridged Guide. Emereo Publishing.

595 Kweon, H., Yoo, M.K., Park, I.K., Kim, T.H., Lee, H.C., Lee, H.-S., Oh, J.-S., Akaike, T., Cho, C.-S., 2003. A
596 novel degradable polycaprolactone networks for tissue engineering. Biomaterials. 24, 801-808.

597 Landis, S.J.M.D.F., 2008. Chronic Wound Infection and Antimicrobial Use. Adv. Skin Wound Care 21,
598 531-540.

599 Lansdown, A.B., Mirastschijski, U., Stubbs, N., Scanlon, E., Agren, M.S., 2007. Zinc in wound healing:
600 theoretical, experimental, and clinical aspects. Wound Repair Regen. 15, 2-16.

601 Lemire, J.A., Harrison, J.J., Turner, R.J., 2013. Antimicrobial activity of metals: mechanisms, molecular
602 targets and applications. Nat. Rev. Micro. 11, 371-384.

603 Li, X., Cui, R., Sun, L., Aifantis, K.E., Fan, Y., Feng, Q., Cui, F., Watari, F., 2014. 3D-Printed Biopolymers
604 for Tissue Engineering Application. Int. J. Polym. Sci. 2014.

605 Liu, Y., He, L., Mustapha, A., Li, H., Hu, Z.Q., Lin, M., 2009. Antibacterial activities of zinc oxide
606 nanoparticles against Escherichia coli O157:H7. J. Appl. Microbiol. 107, 1193-1201.

607 Meaume, S., Teot, L., Lazareth, I., Martini, J., Bohbot, S., 2004. Importance of pain reduction through
608 dressing selection in routine wound management: the MAPP study. J. Wound Care 13, 409-414.

609 Melocchi, A., Parietti, F., Loreti, G., Maroni, A., Gazzaniga, A., Zema, L., 2015. 3D printing by fused
610 deposition modeling (FDM) of a swellable/erodible capsular device for oral pulsatile release of drugs.
611 J. Drug Deliv. Sci. Tec. 30, 360-367.

612 Ng, K.W., Achuth, H.N., Moochhala, S., Lim, T.C., Hutmacher, D.W., 2007. In vivo evaluation of an
613 ultra-thin polycaprolactone film as a wound dressing. J. Biomater. Sci. Polym. Ed. 18, 925-938.

O'Neill, M.A.A., Vine, G.J., Beezer, A.E., Bishop, A.H., Hadgraft, J., Labetoulle, C., Walker, M., Bowler, P.G., 2003. Antimicrobial properties of silver-containing wound dressings: a microcalorimetric study. Int. J. Pharm. 263, 61-68.

Pietrzak, K., Isreb, A., Alhnan, M.A., 2015. A flexible-dose dispenser for immediate and extended release 3D printed tablets. Eur. J. Pharm. Biopharm. 96, 380-387.

Ruparelia, J.P., Chatterjee, A.K., Duttagupta, S.P., Mukherji, S., 2008. Strain specificity in antimicrobial activity of silver and copper nanoparticles. Acta Biomater. 4, 707-716.

Salgado, C.L., Sanchez, E., Mano, J., Moraes, A., 2012. Characterization of chitosan and polycaprolactone membranes designed for wound repair application. J. Mater. Sci. 47, 659-667.

Siddiqui, A.R., Bernstein, J.M., 2010. Chronic wound infection: facts and controversies. Clin. Dermatol. 28, 519-526.

Tenaud, I., Saiagh, I., Dreno, B., 2009. Addition of zinc and manganese to a biological dressing. J. Dermatolog. Treat. 20, 91-94.

Yu, D.G., Zhu, L.M., Branford-White, C.J., Yang, X.L., 2008. Three-dimensional printing in pharmaceutics: Promises and problems. J. Pharm. Sci. 97, 3666-3690.

Zaharia, D.C., Muntean, A.A., Popa, M.G., Steriade, A.T., Balint, O., Micut, R., Iftene, C., Tofolean, I., Popa, V.T., Baicus, C., Bogdan, M.A., Popa, M.I., 2013. Comparative analysis of Staphylococcus aureus and Escherichia coli microcalorimetric growth. BMC microbiology 13, 171.

Zahedi, P., Rezaeian, I., Ranaei-Siadat, S.O., Jafari, S.H., Supaphol, P., 2010. A review on wound dressings with an emphasis on electrospun nanofibrous polymeric bandages. Polymer. Adv. Tech. 21, 77-95.

Figure Captions

Figure 1. Filaments loaded with metals produced, from left to right: plain PCL, Ag (10% w/w)-PCL, Zn (10% w/w)-PCL, Zn (25% w/w)-PCL, Cu (10% w/w)-PCL and Cu (25% w/w)-PCL.

Figure 2. SEM images of: (A) plain PCL, (B) Ag (10% w/w)-PCL, (C) Cu (10% w/w)-PCL, (D) Cu (25% w/w)-PCL, (E) Zn (10% w/w)-PCL and (F) Zn (25% w/w)-PCL.

Figure 3. 3D scan model of a nose (left) and the printed wound dressing of this model with Cu-PCL (right).

Figure 4. FTIR spectra of the 3D printed dressings.

Figure 5. DSC analysis of indicated PCL wound dressings. Exothermic up.

Figure 6. Dissolution profiles of Ag (10% w/w)-PCL, Cu (10% w/w)-PCL, Cu (25% w/w)-PCL, Zn (10% w/w)-PCL and Zn (25% w/w)-PCL in phosphate buffer (pH 7.4).

Figure 7. Growth of *S. aureus* by showing the power generated of bacterial cells vs. time in the presence of increasing amount of dressing containing: (A) control experiments with no PCL or any metal ions, (B) plain PCL, (C) Ag (10% w/w)-PCL, (D) Cu (10% w/w)-PCL, (E) Cu (25% w/w)-PCL, (F) control experiment of plain $CuSO_4$ powder in broth and water without any PCL or bacteria, (G) Zn (10% w/w)-PCL and (H) Zn (25% w/w)-PCL. All experiments were performed at 37 °C over 48 h.

Figure 1

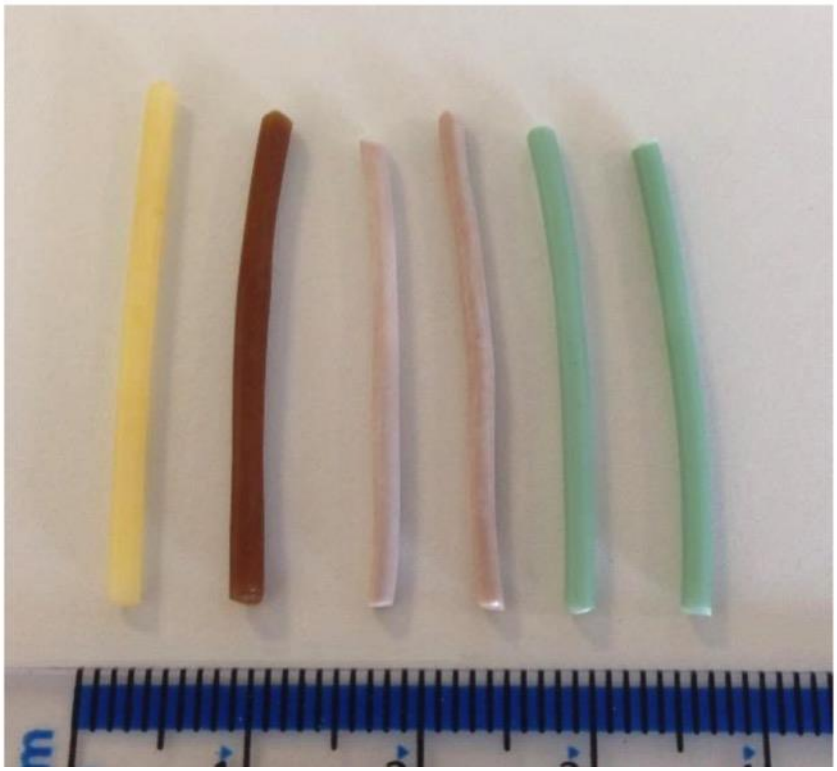

662 ***Figure 2***

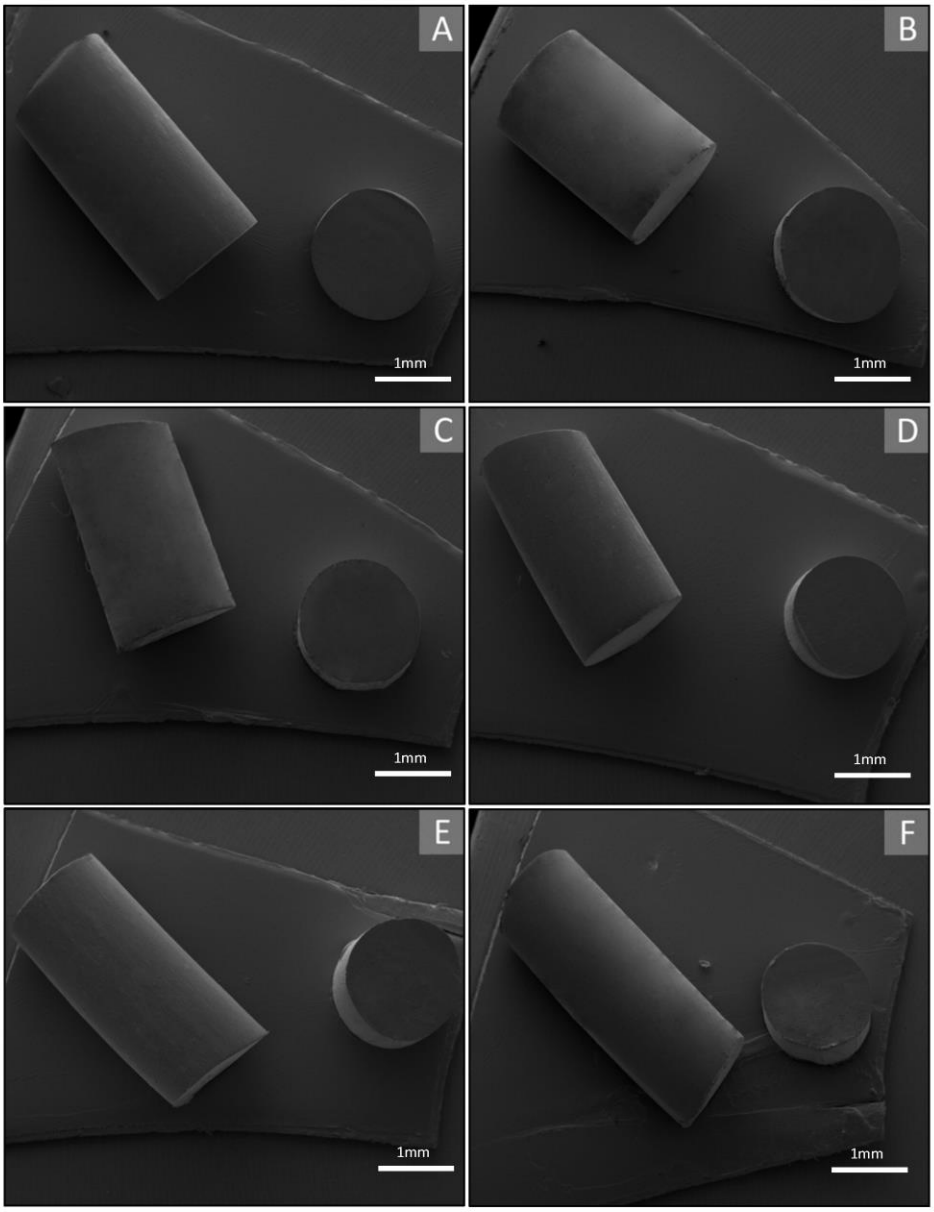

663

664

665 ***Figure 3***

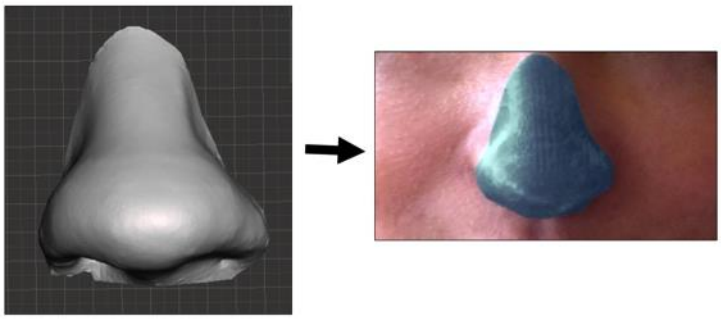

666

667

668 ***Figure 4***

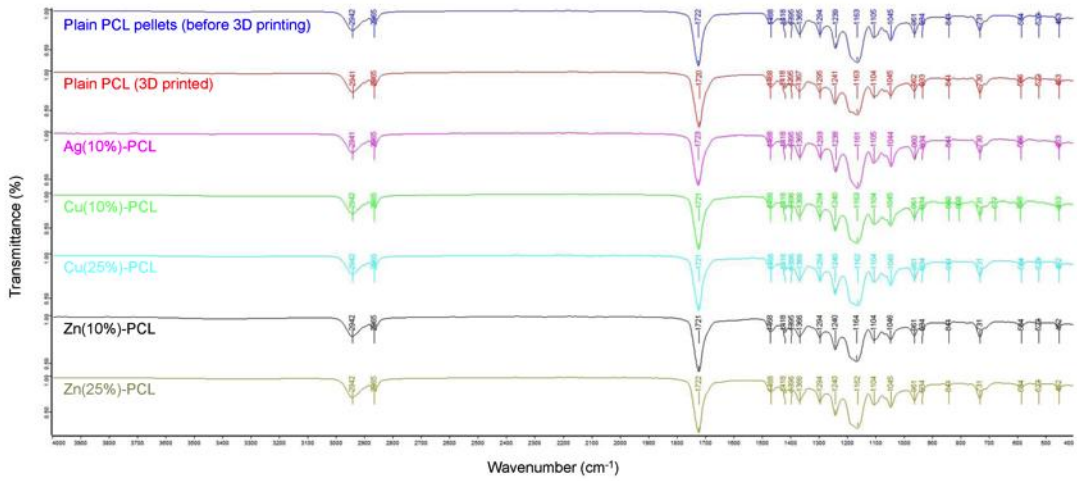

669

670

671

672 ***Figure 5***

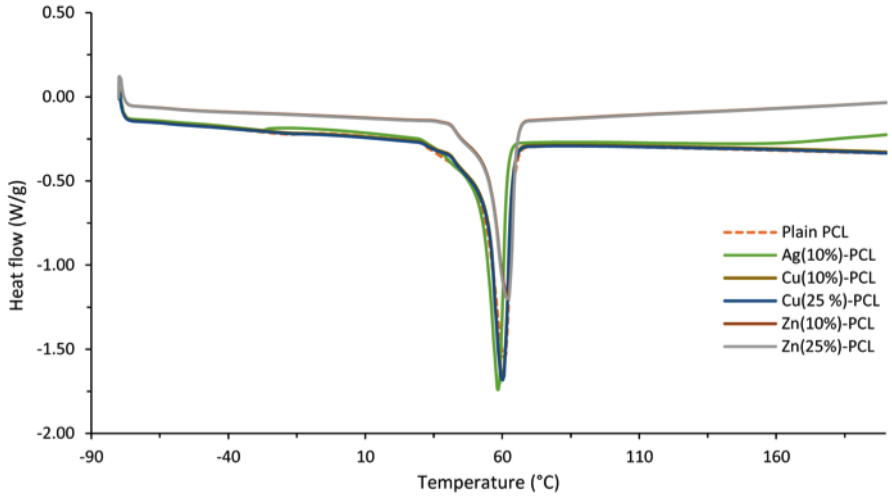

673

674

675 **Figure 6**

676

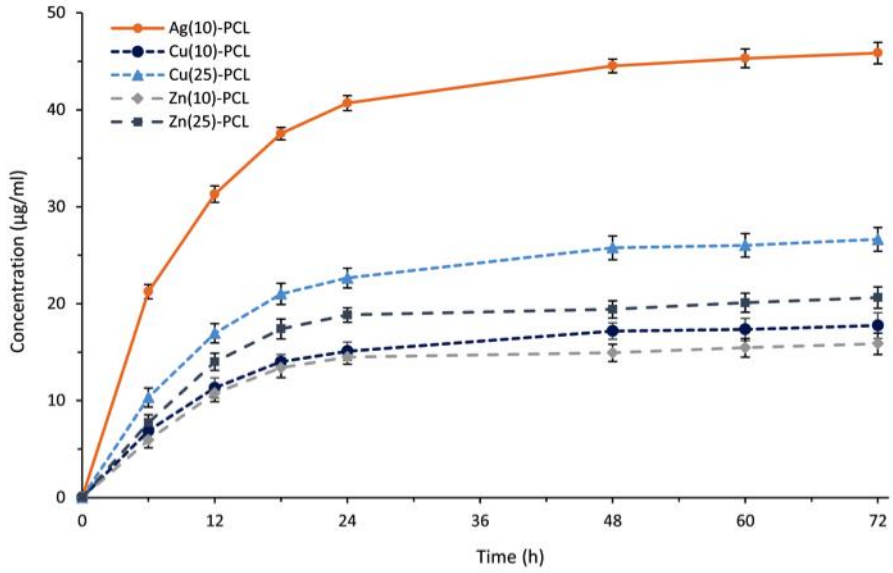

677

678

679 ***Figure 7***

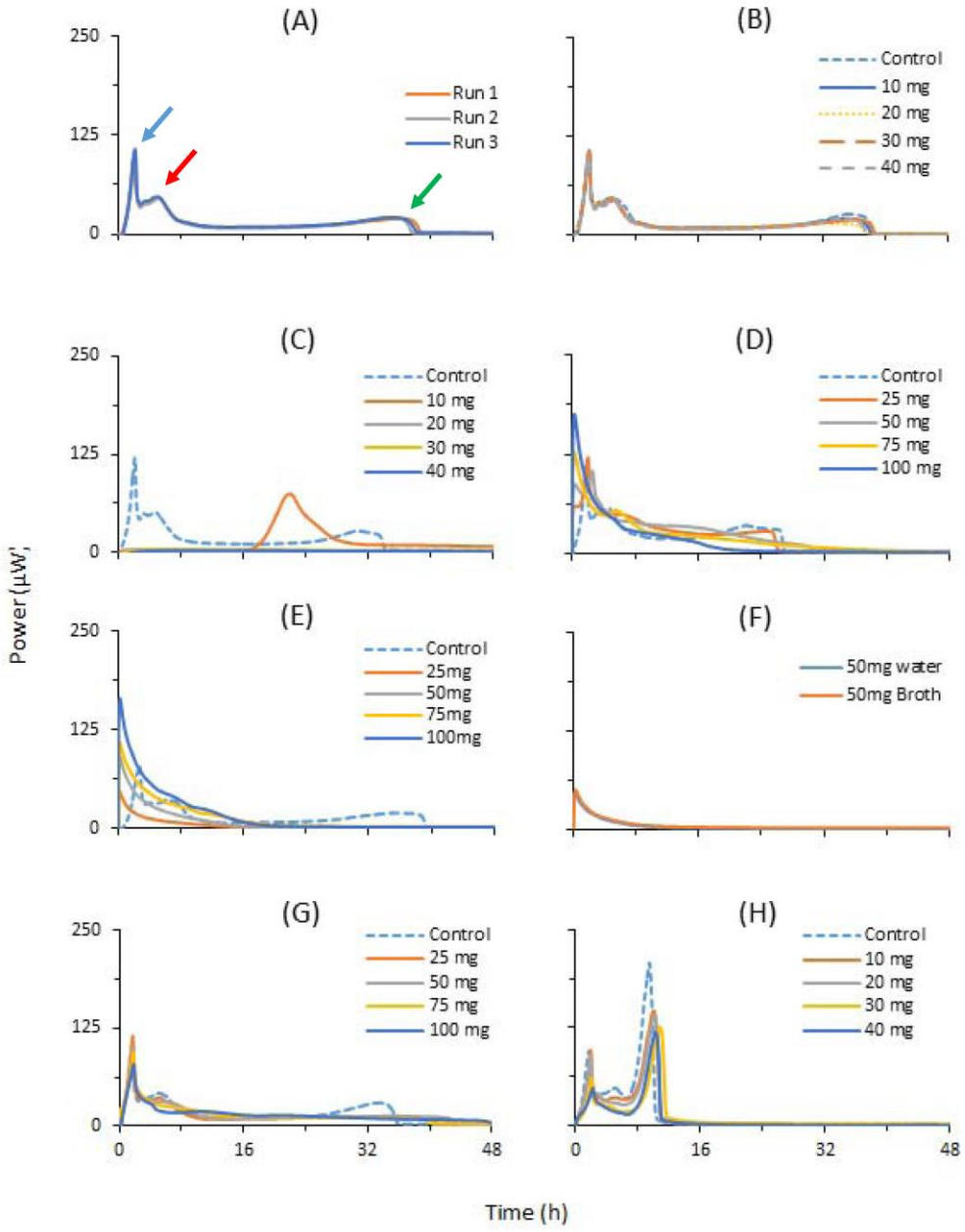

680

681

682 **Appendix 1**

683

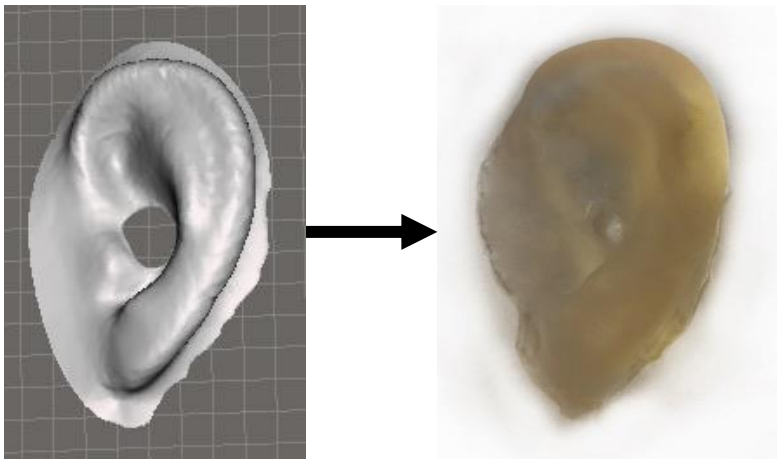

684

685 **Figure 8.** 3D scan model of an ear (left) and the printed wound dressing of this model with Ag-PCL (right).